

2010-07-01

Validated Real-time Energy Models for Small-Scale Grid-Connected PV-Systems

Lacour Ayompe

Technological University Dublin, lacour.ayompe@tudublin.ie

Aidan Duffy

Technological University Dublin, aidan.duffy@tudublin.ie

Sarah McCormack

Trinity College, sarah.mccormack@tcd.ie

See next page for additional authors

Follow this and additional works at: <https://arrow.tudublin.ie/dubenart>



Part of the [Electrical and Electronics Commons](#), [Other Engineering Commons](#), and the [Power and Energy Commons](#)

Recommended Citation

Ayompe, L., Duffy, A., McCormack, S., & Conlon, M. (2010) Validated real-time energy models for small-scale grid-connected PV-systems. *Energy*, vol.36, no.10, pp.4086-4091. doi:10.1016/j.energy.2010.06.021

This Article is brought to you for free and open access by the Dublin Energy Lab at ARROW@TU Dublin. It has been accepted for inclusion in Articles by an authorized administrator of ARROW@TU Dublin. For more information, please contact arrow.admin@tudublin.ie, aisling.coyne@tudublin.ie.



This work is licensed under a [Creative Commons Attribution-NonCommercial-Share Alike 4.0 License](#)
Funder: Department of Education, Ireland

Authors

Lacour Ayompe, Aidan Duffy, Sarah McCormack, and Michael Conlon

Dublin Energy Lab

Articles

Dublin Institute of Technology

Year 2010

Validated real-time energy models for
small-scale grid-connected PV-systems

Lacour Ayompe*

Aidan Duffy†

Sarah McCormack‡

Michael Conlon**

*Dublin Institute of Technology, lacour.ayompe@dit.ie

†Dublin Institute of Technology, aidan.duffy@dit.ie

‡Trinity College, sarah.mccormack@tcd.ie

**Dublin Institute of Technology, Michael.Conlon@dit.ie

This paper is posted at ARROW@DIT.

<http://arrow.dit.ie/dubenart/1>

— Use Licence —

Attribution-NonCommercial-ShareAlike 1.0

You are free:

- to copy, distribute, display, and perform the work
- to make derivative works

Under the following conditions:

- Attribution.
You must give the original author credit.
- Non-Commercial.
You may not use this work for commercial purposes.
- Share Alike.
If you alter, transform, or build upon this work, you may distribute the resulting work only under a license identical to this one.

For any reuse or distribution, you must make clear to others the license terms of this work. Any of these conditions can be waived if you get permission from the author.

Your fair use and other rights are in no way affected by the above.

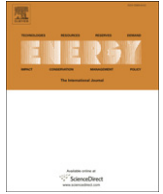
This work is licensed under the Creative Commons Attribution-NonCommercial-ShareAlike License. To view a copy of this license, visit:

- URL (human-readable summary):
<http://creativecommons.org/licenses/by-nc-sa/1.0/>
 - URL (legal code):
<http://creativecommons.org/worldwide/uk/translated-license>
-



Contents lists available at ScienceDirect

Energy

journal homepage: www.elsevier.com/locate/energy

Validated real-time energy models for small-scale grid-connected PV-systems

L.M. Ayompe^{a,*}, A. Duffy^a, S.J. McCormack^b, M. Conlon^c

^a Department of Civil and Structural Engineering, School of Civil and Building Services, Dublin Institute of Technology, Bolton Street, Dublin 1, Ireland

^b Department of Civil, Structural and Environmental Engineering, Trinity College Dublin, Dublin 2, Ireland

^c School of Electrical Engineering Systems, Dublin Institute of Technology, Kevin St, Dublin 8, Ireland

ARTICLE INFO

Article history:

Received 12 January 2010

Received in revised form

15 May 2010

Accepted 19 June 2010

Available online xxx

Keywords:

Real-time

Grid-connected PV-system

Empirical models

Power

Microgeneration

ABSTRACT

This paper presents validated real-time energy models for small-scale grid-connected PV-systems suitable for domestic application. The models were used to predict real-time AC power output from a PV-system in Dublin, Ireland using 30-min intervals of measured performance data between April 2009 and March 2010. Statistical analysis of the predicted results and measured data highlight possible sources of errors and the limitations and/or adequacy of existing models, to describe the temperature and efficiency of PV-cells and consequently, the accuracy of power prediction models. PV-system AC output power predictions using empirical models for PV-cell temperature and efficiency prediction showed lower percentage mean absolute errors (PMAEs) of 7.9–11.7% while non-empirical models had errors of 10.0–12.4%. Cumulative errors for PV-system AC output power predictions were 1.3% for empirical models and 3.3% for non-empirical models. The proposed models are suitable for predicting PV-system AC output power at time intervals suitable for smart metering.

© 2010 Published by Elsevier Ltd.

1. Introduction

A domestic grid-connected PV-system is a type of installation where three major components are used: the PV-generator (comprising a number of PV-modules connected in series or parallel on a mounting structure); the inverter; DC and AC cabling and a conventional power line [1,2]. Inverters play a key role in energy efficiency and reliability since they operate the PV-array at the Maximum Power Point (MPP). Moreover, inverters convert the DC power generated by PV-modules into alternating current (AC) of the desired voltage and frequency (e.g. 230 V/50 Hz). Installations of this type do not include batteries [3,4].

Most existing generic models for assessing the energy output of PV-systems are lumped since they determine average daily, monthly or annual energy output. These models are adapted to support policies such as net metering (applicable in Japan and some States in America) where electricity is sold to the grid at the same price at which it is bought. Lumped models are also useful in countries where enhanced feed-in tariffs (high buy-back rates) apply such as in Germany, Spain, Italy, Greece and France. Lumped models are, however, not adapted to analyse the real-time or dynamic performances of grid-connected PV-systems such as those where support policies are based on paying for the excess (or spill)

electricity generated, which is fed into the utility grid (such as in other countries and Ireland). Moreover, they cannot cope with variable electricity prices based on time of use, which is likely to become more common as smart metering becomes widely deployed.

Smart meters provide much more precise information on electricity consumed as well as the time of use. They are intelligent two-way communication devices with digital real-time power measurement. They offer the opportunity for remote operation and remote meter reading as well as the potential for real-time pricing, new tariff options and demand side management.

During the day when solar radiation is available, a grid-connected PV-system generates AC power. If the PV-system is installed in a domestic dwelling, the AC power is fed into the main electrical distribution panel of the house from which it can provide power to the house for on-site consumption, the excess is supplied to the utility grid. Fig. 1 shows representative plots of measured electricity generated from a 1.72 kW_p PV-system located in Dublin, Ireland, average electricity consumption of a representative domestic dwelling in Ireland and the quantity of electricity exported and spilled to the grid on the 1st of June 2009.

The objective of this paper therefore, is, to develop a validated real-time mathematical model that predicts the electricity output of small-scale grid-connected PV-systems. The model can be used to generate time-stepped output data, which can be combined with domestic demand data to predict the quantity of on-site electricity consumption based on different users' demand profiles.

* Corresponding author. Tel: +353 14023940; fax: +353 14022997.

E-mail address: lacour.ayompe@dit.ie (L.M. Ayompe).

Nomenclature

A	area (m ²)
AM	air mass
C	heat capacity (JK ⁻¹)
G _m	in-plane solar radiation (W m ⁻²)
h _c	forced convective heat transfer coefficient (Wm ⁻² K ⁻¹)
h _{c,w}	convective heat transfer coefficient due to wind (Wm ⁻² K ⁻¹)
h _r	radiative heat transfer coefficient (Wm ⁻² K ⁻¹)
n _m	number of modules
Q _G	absorbed solar radiation (W)
Q _r	thermal losses by radiation (W)
Q _c	thermal losses by convection (W)
NOCT	normal operating cell temperature (45 °C)
P _{el}	electrical power (W)
T	temperature (°C)
U _L	overall heat transfer coefficient (Wm ⁻² K ⁻¹)
V _w	wind speed (m s ⁻¹)
PMAE	percentage mean absolute error (%)

Subscripts

a	ambient
AC	alternating current
c	PV-cell
DC	direct current
inv	inverter
m	module
MPP	maximum power point
n,c	nominal cell
PV	photovoltaic
r	reference
STC	standard test condition
w	wind

Greek symbols

α	absorptivity
β	temperature coefficient of P _m of the PV-panel (0.003 °C ⁻¹)
η	efficiency (%)
τ	transmissivity
σ	Stefan–Boltzman's constant (5.67 × 10 ⁻⁸ Wm ⁻² K ⁻⁴)
ε	emissivity

2. PV output modelling

PV output modelling involves identifying all independent variables and establishing their mathematical relationships with power output. The variables identified include solar radiation; wind speed; ambient temperature; cell efficiency; cell temperature and module area.

Given that current smart metering practice is based on 30-min intervals, the mathematical representation of the PV-system was simulated at 30-min intervals daily using measured data between April 2009 and March 2010. In order to achieve this, it is necessary to accurately predict the PV-cell temperature, which influences the cell efficiency. Once the cell efficiency and inverter efficiency at any given instant are accurately predicted, the PV-power equation is then used to calculate the power output from the PV-system.

2.1. PV-cell temperature

The temperature of PV-cells is one of the most important parameters used in assessing the performance of PV-systems and

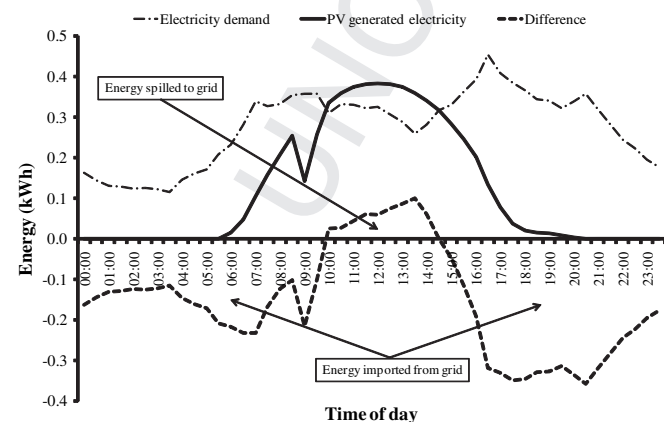


Fig. 1. Representative daily domestic scale PV-system electricity generation and demand.

their electricity output. The cell temperature depends on several parameters such as the thermal properties of the materials used, type of cells, module configuration and local climate conditions [5,6].

A PV-module's efficiency strongly depends on its cells' operating temperature. PV-cell temperatures are very difficult to measure since the cells are tightly encapsulated in order to protect them from environmental degradation. The temperature of the back surface of PV-modules is commonly measured and used in place of the cell temperature with the assumption that these temperatures closely match [7].

From a mathematical point of view, correlations for PV-cell operating temperature (T_c) are either explicit in form, thus giving T_c directly, or implicit, i.e. involve variables such as cell efficiency or heat transfer coefficients, which themselves depend on T_c . In the latter case, an iteration procedure is necessary to calculate the cell temperature [8]. Six models for PV-cell temperature evaluation were identified from literature. They include five explicit and one implicit model, the latter comprising of a steady-state model.

2.1.1. Explicit correlations

The explicit correlation models express the PV-cell temperature as a function of ambient temperature, solar radiation, wind speed and other system parameters ignoring heat exchange dynamics between the module and its environment. The first correlation expresses the cell temperature of a PV-module T_c in Eq. (1) as [9]:

$$T_c = T_a + \frac{G_m}{800}(\text{NOCT} - 20) \left(1 - \frac{\eta_c}{\tau\alpha}\right) \quad (1)$$

where, $\tau\alpha = 0.9$ [10].

A simplified model of Eq. (1) is given in Eq. (2) as [11,12]:

$$T_c = T_a + \frac{G_m}{800}(\text{NOCT} - 20) \quad (2)$$

Eq. (3) gives the simplest explicit correlation for the operating temperature of a PV-cell with the ambient temperature and incident solar radiation flux [8]. Earlier reported values for h_w were in the range 0.02–0.04 Wm⁻²K⁻¹ [13]. In this study, h_w was determined to be 0.018 Wm⁻²K⁻¹ using nonlinear regression analysis on measured data.

$$T_c = T_a + G_m h_w \quad (3)$$

where, T_c and T_a are in degrees Kelvin.

The PV-module temperature can also be determined using Eq. (4) proposed by Tamizh Mani et al. in [14] given as:

$$T_c = a + bG_m + cT_a + dV_w \quad (4)$$

where, a , b , c and d are system-specific regression coefficients with values of -1.987 , 0.02 , 1.102 and -0.097 , respectively, and R^2 of 0.97 determined using measured data from the Dublin site.

King in [8] proposed an expression for PV-cell temperature given by Eq. (5) as:

$$T_c = T_a + \frac{G_m}{G_{STC}} [aV_w^2 + bV_w + c] \quad (5)$$

where, a , b , and c are coefficients with values of 0.043 , -1.652 and 24.382 , respectively, and R^2 of 0.96 , again determined using measured data.

Other explicit correlations reported in literature [8] are based on field performance data, which are site specific and, therefore, not applicable in this case.

2.1.2. Steady-state analysis

In this approach it is assumed that, within a short-time period (normally less than 1 h), the intensity of the incoming solar irradiance and other parameters affecting the PV-module's behaviour are constant. If the variation in the overall heat loss rates of the PV-module is small, then it can be assumed that the rate of heat transfer from the PV-module to the environment is steady and the temperatures at each point of the PV-module are constant over a short-time period [7].

The equation for the PV-cell temperature operating under steady state is derived assuming that the incident energy on a solar cell is equal to the electrical energy output of the cell plus the sum of the energy losses due to convection and radiation. The resulting energy balance equation is given as [15,16]:

$$\dot{Q}_G - P_{el} - \dot{Q}_r - \dot{Q}_c = 0 \quad (6)$$

Substituting the relevant terms in Eq. (6) results in Eq. (7) given as [17]:

$$\tau\alpha G_m A_c - \eta_c G_m A_c - 2h_r A_c (T_c - T_a) - 2h_c A_c (T_c - T_a) = 0 \quad (7)$$

From Eq. (5), the PV-module temperature is given as:

$$T_c = \frac{(\tau\alpha - \eta_{PV})G_m}{2(h_r + h_c)} + T_a \quad (8)$$

where, T_c and T_a are in degrees Kelvin.

2.1.3. Heat transfer coefficients

The radiative heat transfer coefficient between the module front and the sky, and the module rear and the ground (h_r) is given as [18]:

$$h_r = \sigma\epsilon(T_c^2 + T_a^2)(T_c + T_a) \quad (9)$$

The convective heat flow is dominated at the module front by forced convection driven by wind forces and at the module rear, depending on the installation situation, by free laminar or turbulent convection. The convective heat transfer coefficient is given as [17]:

$$h_c = \sqrt[3]{h_{c,w}^3 + h_{c,free}^3} \quad (10)$$

$$h_{c,w} = 4.214 + 3.575V_w \quad (11)$$

$$h_{c,free} = 1.78(T_c - T_a)^{1/3} \quad (12)$$

Because of the wide discrepancies in the value for h_c , it is difficult to choose a particular value. Duffie and Beckman [18] suggested the use of the expression for $h_{c,w}$ proposed by McDamms [19] for flat plates exposed to outside winds:

$$h_{c,w} = 5.67 + 3.86V_w \quad (13)$$

Nolay in [10] uses the following relationship:

$$h_{c,w} = 5.82 + 4.07V_w \quad (14)$$

2.2. PV-cell and module efficiency

The most widely known model to predict the efficiency of a PV-cell (η_c) is given as [10,20]:

$$\eta_c = \eta_{n,c} [1 - \beta(T_c - T_r) + \gamma \log(G_m/1000)] \quad (15)$$

where, $T_r = 25^\circ\text{C}$, $\gamma = 0.12$.

Most often Eq. (15) is given with $\gamma = 0$ and it reduces to a linear dependence of η_c on temperature given as [10,16]:

$$\eta_c = \eta_{n,c} [1 - \beta(T_c - 25)] \quad (16)$$

The efficiency of solar cells can also be expressed as being dependent on the incident solar radiation and cell temperature. The efficiency at a particular irradiance or temperature is the result of the nominal efficiency minus the change in efficiency given as [2]:

$$\eta_c = \eta_{n,c} \left[1 + \beta \ln \left(\frac{G_m}{1000} \right) - \beta(T_c - 25) \right] \quad (17)$$

Another expression for the cell efficiency assuming that the transmittance-absorbance losses ($\tau\alpha/U_L$) are constant over the relevant operating temperature range is given as [21]:

$$\eta_c = \eta_{n,c} \left[1 - 0.9\beta \frac{G_m}{800} (\text{NOCT} - 20) - \beta(T_a - 25) \right] \quad (18)$$

Durisch et al. [22] developed a semi-empirical PV-cell efficiency model given as:

$$\eta_c = \eta_{n,c} a \left[b \frac{G_m}{G_0} + \left(\frac{G_m}{G_0} \right)^c \right] \left[d + e \frac{T_c}{T_r} + f \frac{\text{AM}}{\text{AM}_0} + \left(\frac{\text{AM}}{\text{AM}_0} \right)^g \right] \quad (19)$$

where, $G_0 = 1000 \text{ Wm}^{-2}$, $T_r = 25^\circ\text{C}$, $\text{AM}_0 = 1.5$.

The parameters a , b , c , d , e , f and g are regression coefficients with values of 1.249 , -0.241 , 0.193 , 0.244 , -0.179 , -0.037 and 0.073 , respectively, and R^2 of 0.99 which were determined using measured data from the Dublin site. The air mass (AM) is the ratio of the mass of air that the direct radiation has to traverse at any given time and location to the mass of air that it would traverse if the sun were at the zenith [23]. The air mass is calculated for any time of day at any day of the year from the sun's altitude Φ (in degrees) using the equation given as [24]:

$$\text{AM} = 1/\cos(90 - \Phi) \quad (20)$$

The nominal efficiency ($\eta_{n,c}$) of PV-cells is given as [2]:

$$\eta_{n,c} = \frac{P_{\text{MPP(StC)}}}{A_c \times G_{\text{STC}}} \quad (21)$$

The nominal efficiency of a PV-module is given as:

$$\eta_{n,m} = \eta_{n,c} \times \text{PF} \quad (22)$$

The pack factor (PF) is the ratio of the total area of PV-cells (A_c) over the area of the PV-module (A_m) and is given as [12]:

Table 1
Percentage mean absolute error (PMAE) for PV-cell temperature predictions.

	Eq. (1)	Eq. (2)	Eq. (3)	Eq. (4)	Eq. (5)	Eq. (8)
PMAE	14.4	23.3	8.2	7.3	7.1	8.8

$$PF = \frac{A_c}{A_m} \quad (23)$$

The measured PV-module efficiency is given as [18]:

$$\eta_{exp} = \frac{V_{DC}I_{DC}}{G_m A_m} \quad (24)$$

2.3. PV-array power output

The DC power output from a PV-array is given as:

$$P_{DC} = n_m \times \eta_{n,c} \times \eta_L \times PF \times G_m \times A_m \quad (25)$$

η_L accounts for losses that reduce power output from standard test conditions (STCs). These losses include the difference of the operating PV-cell temperature from the standard 25 °C, the deviation from the maximum power point, the ohmic losses of the conductors, the cleanness of the PV-module surface, the deviation of the solar irradiance from an ideal path in order to produce a photoelectron in the cell (optical path deviation), the aging of the PV material, etc [25]. Kaushika and Rai [26] investigated mismatch losses in solar photovoltaic cell networks while Mavromatakis et al. [25] presented expressions for reflection and difference in operating PV-cell temperature losses. Due to the complexity of modelling the individual losses, η_L is often modelled using Eqs. (15)–(19) representing the terms that are multiplied by the nominal PV-cell efficiency ($\eta_{n,c}$). Eq. (25) therefore reduces to

$$P_{DC} = n_m \times \eta_c \times PF \times G_m \times A_m \quad (26)$$

2.4. Inverter efficiency

The inverter efficiency is given as [9]:

$$\eta_{inv} = \frac{P_{inv,n}}{P_{PV,n}} \quad (27)$$

The normalised inverter output $P_{inv,n}$ is given as a second-order polynomial by Peippo and Lund in [9] as:

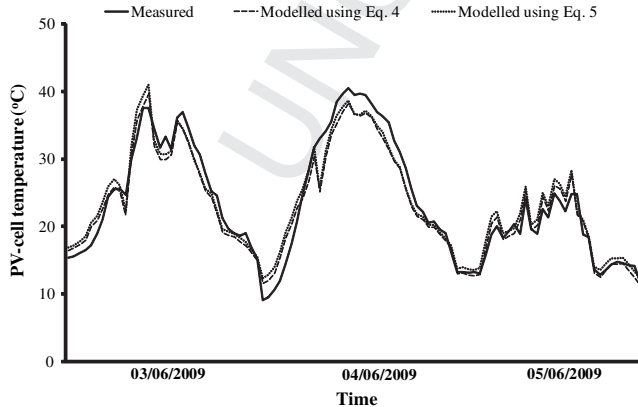


Fig. 2. Measured and modelled PV-cell temperature.

Table 2
PMAE for predicted PV-array power output.

	Eq. (1)	Eq. (2)	Eq. (3)	Eq. (4)	Eq. (5)	Eq. (8)
Eq. (15)	9.1	11.6	9.8	9.7	9.9	10.2
Eq. (16)	12.5	15.4	13.4	13.3	13.4	13.8
Eq. (17)	12.3	15.2	13.2	13.1	13.2	13.5
Eq. (18)	11.4	12.0	11.2	11.3	11.3	11.5
Eq. (19)	7.8	11.0	7.3	7.3	7.7	8.3

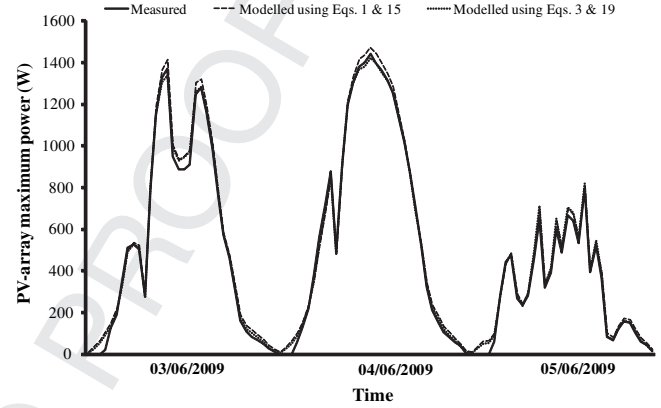


Fig. 3. Measured and modelled PV-array maximum DC power output.

$$P_{inv,n} = k_0 + k_1 P_{PV,n} + k_2 P_{PV,n}^2 \quad (28)$$

where

$$P_{PV,n} = \frac{P_{PV}}{P_{inv,rated}} \quad (29)$$

and

$$P_{inv,n} = \frac{P_{inv}}{P_{inv,rated}} \quad (30)$$

k_0 is the normalised self-consumption loss, k_1 is the linear efficiency coefficient and k_2 is the coefficient for losses proportional to input power squared as defined by Peippo and Lund in [9]. $P_{PV,n}$ and $P_{inv,n}$ are the normalised inverter input and output power, respectively. P_{PV} and P_{inv} are the PV-array DC input and AC output from the inverter at any instant of time, respectively, while $P_{inv,rated}$ is the rated inverter input capacity. A regression analysis carried out on normalised inverter input and output power yielded values for the constants k_0 , k_1 and k_2 of -0.001 , 0.926 and 0.004 , respectively with R^2 of 1.

2.5. PV-system power output

The PV-system AC power output is given as:

$$P_{AC} = \eta_{inv} P_{DC} \quad (31)$$

Table 3
Percentage cumulative error for predicted PV-array output energy.

	Eq. (1)	Eq. (2)	Eq. (3)	Eq. (4)	Eq. (5)	Eq. (8)
Eq. (15)	2.5	6.5	3.8	3.8	3.8	4.2
Eq. (16)	8.0	12.1	9.4	9.4	9.4	9.7
Eq. (17)	7.7	11.8	9.1	9.0	9.0	9.4
Eq. (18)	3.3	7.3	4.6	4.6	4.6	5.0
Eq. (19)	2.3	6.7	0.7	0.6	0.6	1.4

Table 4

PMAE for predicted PV-system AC output power.

	Eq. (1)	Eq. (2)	Eq. (3)	Eq. (4)	Eq. (5)	Eq. (8)
Eq. (15)	10.0	12.4	10.7	10.6	10.7	11.1
Eq. (19)	8.4	11.7	7.9	7.9	8.3	9.0

3. Modelling

MatLab software was used to develop a programme to predict the energy output from a trial PV installation using measured weather data at 30-min intervals between April 2009 and March 2010. At every given instant, the PV-cell temperature was modelled using Eqs.(1)–(5) and (8). PV-array DC power and PV-system AC power outputs were modelled using Eqs. (26) and (31), respectively.

3.1. PV-system description

The PV-system used to validate the above models consisted of a 1.72 kW_p PV-array composed of 8 modules covering a total area of 10 m² installed on a flat roof at the Focas Institute building, Dublin Institute of Technology, Dublin, Ireland. The 215 W_p Sanyo HIP-215NHE5 PV-modules are made of thin monocrystalline silicon wafer surrounded by ultra-thin amorphous silicon layers with anti-reflective coatings that maximized sunlight absorption [27]. The unshaded modules were installed facing due south and inclined at 53° to the horizontal corresponding to the local latitude of the location. The roof was approximately 12 m high and the modules were mounted on metal frames that were 1 m high.

A 1700 W AC power single-phase Sunny Boy inverter was installed to convert the DC electricity from the PV-array to AC that was fed into the 220–240 V AC electrical network of the building. The data acquisition system consisted of a Sunny Boy 1700 inverter, Sunny SensorBox and Sunny WebBox. The Sunny SensorBox was used to measure in-plane global solar radiation on the PV-modules. Additional sensors for measuring ambient temperature, wind speed and temperature at the back of the PV-module were connected to the SensorBox. The SensorBox and the inverter were connected to the Sunny WebBox via a serial RS485 link and a Power Injector. Data was recorded at 5-minute intervals using the WebBox.

3.2. Data and results comparison

In order to quantify variations between predicted and measured values, percentage mean absolute error (PMAE) was used. It evaluates the percentage mean of the sum of absolute deviations arising due to both over-estimation and under-estimation of individual observations. PMAE is given as:

$$\text{PMAE} = \frac{1}{N} \sum_{i=1}^N \left[\frac{(C_i - M_i)^2}{M_i} \right]^{\frac{1}{2}} \times 100\% \quad (33)$$

N is the total number of observations while C_i and M_i are the i th calculated and measured values, respectively.

3.3. Weather data

One year's data collected at 5-min intervals between April 2009 and March 2010 at the test site was aggregated to 30 min and used for model validation. The data composed of solar radiation, ambient temperature, PV-module temperature, wind speed, PV-array DC current, PV-array DC voltage and PV-system AC power output.

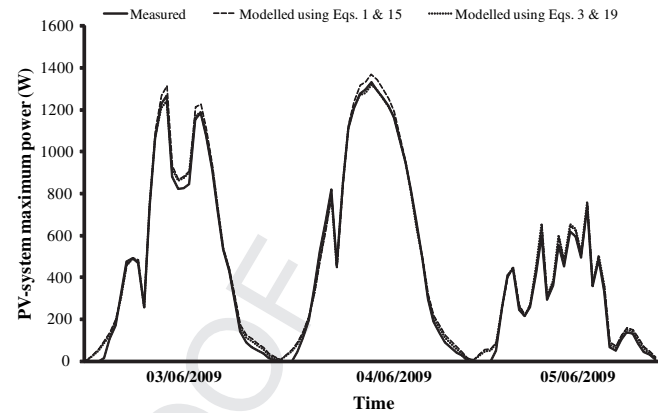


Fig. 4. Measured and modelled PV-system maximum AC power output.

The monthly average daily total solar insolation varied between 1.11 kWh/m²/day in December and 4.57 kWh/m²/day in June while the annual total measured in-plane solar insolation was 1043.1 kWh/m². The monthly average daily wind speed varied between 2.5 m/s in February and 6.6 m/s in November. The monthly average ambient temperature varied between 6.0 °C in January and 18.8 °C in August while the PV-module temperature varied between 8.8 °C in January and 23.8 °C in June. Maximum recorded values for solar radiation, ambient temperature, PV-module temperature and wind speed were 1031.0 Wm⁻², 27.0 °C, 45.8 °C and 16.3 ms⁻¹ in August, June, September and November, respectively.

4. Results and discussions

4.1. PV-cell temperature

Table 1 presents PMAE for PV-cell temperature predictions using the models in Eqs. (1)–(5) and (8). The results show that the empirical models in Eqs. (4) and (5) produce the least PMAE of 7.3% and 7.1%, respectively. Where field trial data is not available to derive the empirical coefficients, Eq. (1) can be used to predict the PV-cell temperature with a higher PMAE of 14.4%. Fig. 2 shows plots of measured and modelled PV-cell temperature using Eqs. (4) and (5). It can be seen from Fig. 2 that the predicted PV-cell temperatures show good correlation with the measured data.

4.2. PV-array output power

PMAE for predicted PV-array DC power output using PV-cell temperature models (Eqs. (1)–(5) and (8)) and modified PV-cell efficiency models (Eqs. (15)–(19)) are presented in Table 2. The results show that when field trial data is available to obtain regression coefficients, the empirical models for PV-cell temperature (Eqs. (3) and (4)) and PV-cell efficiency (Eq. (19)) yield the lowest PMAE of 7.3%. Where only weather data is available, Eqs. (1) and (15) can be used to predict PV-array output power with PMAE of 9.1%. Fig. 3 shows plots of measured and modelled PV-array maximum DC output power. It can be seen that the predicted PV-array maximum output power shows good correlation with the measured data.

Table 5

Percentage cumulative error for predicted PV-system AC output energy.

	Eq. (1)	Eq. (2)	Eq. (3)	Eq. (4)	Eq. (5)	Eq. (8)
Eq. (15)	3.3	7.4	4.6	4.6	4.6	5.0
Eq. (19)	-1.6	7.5	1.4	1.3	1.4	2.2

Table 3 shows percentage cumulative errors for predicted PV-array output energy against the measured power output of 1661.4 kWh. The empirical models in Eqs. (3)–(5) and (19) have percentage cumulative errors of 0.6–0.7% while the non-empirical models using Eqs. (1) and (15) have an error of 2.5%. Both models, however, tend to over-estimate PV-array power output during sunrise.

4.3. PV-system AC output power

PMAE for PV-system AC power prediction using modelled PV-cell temperatures (Eqs. (1)–(5) and (8)) and PV-cell efficiency (Eqs. (15)–(19)) are shown in Table 4. The empirical models (Eqs. (3), (4) and (9)) give the lowest PMAE of 7.9% while the non-empirical models (Eqs. (1) and (15)) yield a PMAE of 10%. Again the results show that more accurate predictions are obtained when measured PV-system performance data are used to generate empirical models. Fig. 4 shows measured and modelled PV-system AC output power. It is seen in Fig. 4 that both the empirical and non-empirical models show good agreement with measured data.

Table 5 presents percentage cumulative errors for PV-system AC energy output prediction using PV-cell temperature models (Eqs. (1)–(5) and (8)) and PV-cell efficiency models (Eqs. (15) and (19)) against the measured PV-system AC energy output of 1522.5 kWh. The empirical models (Eqs. (3)–(5) and (19)) result in over-estimations of 1.3–1.4% while the non-empirical models (Eqs. (1) and (15)) have an over-estimation error of 3.3%.

5. Conclusions

Introduction of smart meters in countries such as Ireland, Belgium and the UK which are currently trailing this technology with a view of its widespread deployment necessitates more accurate prediction of PV-system power output within short-time intervals such as 30 min. In this study, measured field performance data for a domestic-scale grid-connected PV installation was used to validate some of the widely quoted correlations in literature employed to model PV-cell temperature and efficiency for power output prediction. The best prediction of PV-system AC output power was obtained using Eq. (4) for PV-cell temperature and Eq. (19) for PV-cell efficiency with percentage mean absolute and cumulative errors of 7.9% and 1.3%, respectively. Results show that for short-term PV-array power output prediction as is applicable to smart metering, two options are available.

- Where field performance data of the PV-system is available, empirical models for PV-cell temperature (Eqs. (3) and (4)) and PV-cell efficiency (Eq. (19)) are to be used.
- Where field performance data of the PV-system is not available, the non-empirical models for PV-cell temperature (Eq. (1)) and PV-cell efficiency (Eq. (15)) are to be used.

In both cases, inverter performance data is required to model the PV-system AC power output. The proposed models should help

to establish the dynamic performance of PV-systems when combined with time-of-day billing systems.

References

- [1] Spooner ED, Harbidge G. Review of international standards for grid connected photovoltaic systems. *Renew Energy* 2001;22(1-3):235–9.
- [2] The German Solar Energy Society. Planning and installing photovoltaic systems: a guide for installers, architects and engineers. UK: James and James; 2006.
- [3] Cramer G, Ibrahim M, Keinkauf W. PV system technologies: state-of-the-art and trends in decentralized electrification. Refocus; January/February 2004.
- [4] Bernal-Aguistin JL, Dufo-López R. Economical and environmental analysis of grid connected photovoltaic systems in Spain. *Renew Energy* 2006;31(8):1107–28.
- [5] Alonso García MC, Balenzategui JL. Estimation of photovoltaic module yearly temperature and performance based on nominal operation cell temperature calculations. *Renew Energy* 2004;29(12):1997–2010.
- [6] Jones AD, Underwood CP. A thermal model for photovoltaic systems. *Solar Energy* 2001;70(4):349–59.
- [7] Trinuruk P, Sorapipatana C, Chenvidhya D. Estimating operating cell temperature of BIPV modules in Thailand. *Renew Energy* 2009;34(11):2515–23.
- [8] Skoplaki E, Palyvos JA. Operating temperature of photovoltaic modules: a survey of pertinent correlations. *Renew Energy* 2009;34(1):23–9.
- [9] Mondol JD, et al. Long-term validated simulation of a building integrated photovoltaic system. *Solar Energy* 2005;78(2):163–76.
- [10] Mattei M, et al. Calculation of the polycrystalline PV module temperature using a simple method of energy balance. *Renew Energy* 2006;31(4):553–67.
- [11] Kymakis E, Kalykakis S, Papazoglou TM. Performance analysis of a grid connected photovoltaic park on the island of Crete. *Energy Convers Manage* 2009;50(3):433–8.
- [12] Markvart T, editor. *Solar electricity*. 2nd ed. , Chichester: John Wiley and Sons; 2000.
- [13] Buresch M. *Photovoltaic energy systems*. , New York: McGraw-Hill; 1983.
- [14] Chenni R, et al. A detailed modeling method for photovoltaic cells. *Energy* 2007;32(9):1724–30.
- [15] Ueda Y, et al. Performance analysis of various system configurations on grid-connected residential PV systems. *Solar Energy Mater Solar Cells* 2009;93(6-7):945–9.
- [16] Kolhe M, et al. Analytical model for predicting the performance of photovoltaic array coupled with a wind turbine in a stand-alone renewable energy system based on hydrogen. *Renew Energy* 2003;28(5):727–42.
- [17] Eicker U. *Solar technologies for buildings*. England: John Wiley and Sons; 2003.
- [18] Duffie JA, Beckman WA. *Solar engineering of thermal processes*. , New York: Wiley; 1991.
- [19] McAdams WC, editor. *Heat transmission*. 3rd ed. , New York: McGraw-Hill; 1954.
- [20] Cucumo M, et al. Performance analysis of a 3 kW grid-connected photovoltaic plant. *Renew Energy* 2006;31(8):1129–38.
- [21] Hove T. A method for predicting long-term average performance of photovoltaic systems. *Renew Energy* 2000;21(2):207–29.
- [22] Durisch W, et al. Efficiency model for photovoltaic modules and demonstration of its application to energy yield estimation. *Solar Energy Mater Solar Cells* 2007;91(1):79–84.
- [23] Kalogirou SA. *Solar energy engineering: processes and systems*. , London: Elsevier; 2009.
- [24] Durisch W, Lam KH, Close J. Efficiency and degradation of a copper indium diselenide photovoltaic module and yearly output at a sunny site in Jordan. *Appl Energy* 2006;83(12):1339–50.
- [25] Mavromatakis F, et al. Modeling the photovoltaic potential of a site. *Renew Energy* 2009;35(7):1387–90.
- [26] Kaushika ND, Rai AK. An investigation of mismatch losses in solar photovoltaic cell networks. *Energy* 2007;32(5):755–9.
- [27] Sanyo HIT photovoltaic module manual for HIP-215NHE5, HIP-210NHE5 and HIP-205NHE5. Available from: <http://www.solarcentury.com/Residential-developers/Specifying-Solar/PV-Catalogue/HIP-215-NHE5-NHE-Series>.